Original Paper

phys. stat. sol. (a) **203**, No. 7, 1513–1520 (2006) / **DOI** 10.1002/pssa.200563108

Influence of substrate treatment on the growth morphology and magnetic anisotropy of epitaxial CrO_2 films

Guo-Xing Miao[*, 1, 2], **Gang Xiao**[2], and **Arunava Gupta**[1]

[1] Center for Materials for Information Technology, University of Alabama, Tuscaloosa, Al 35487, USA
[2] Physics Department, Brown University, Providence, RI 02912, USA

Received 5 July 2005, accepted 1 March 2006
Published online 22 May 2006

PACS 75.30.Gw, 75.60.Jk, 75.70.Ak, 81.05.Bx, 81.15.Gh

Epitaxial CrO_2 thin films deposited on HF-cleaned TiO_2(100) substrates exhibit very strong strain anisotropy, while those grown without the HF treatment step are essentially strain-free and display bulk-like magnetic properties. The HF treatment enhances the surface smoothness of the TiO_2(100) substrate thus leading to the growth of epitaxially strained CrO_2 films. The magnetic easy axis of these films changes orientation with thickness, switching from the in-plane *c*-axis direction for relatively thick films to the *b*-axis direction for thinner films (<50 nm). Similarly, over a thickness range, a change of the easy axis direction is also observed with lowering temperature. Ion-beam irradiation of the substrate surface prior to growth also results in the growth of strained CrO_2 films, although the amount of strain is less than that observed for HF-treated substrates. The magnetic properties as a function of thickness have also been studied for as-deposited 'thick' CrO_2 films that are slowly chemically etched down in thickness. Unlike as-grown thin films below 50 nm thickness that have the easy axis along the *b*-direction, the chemically etched down CrO_2 thin films of equivalent thickness retain their easy axis alignment along the *c*-direction, but display a significantly enhanced coercivity. The observed differences in the switching behavior between the as-deposited films and those that are chemically etched can be qualitatively attributed to changes in the strain relaxation mechanism.

1 Introduction

There has been much interest in recent years in studying the magnetotransport properties of chromium dioxide (CrO_2) because of its potential application in the emerging field of spintronics. Band structure calculations have shown that CrO_2 is a half-metallic material, i.e. it contains a gap in the minority spin channel at the Fermi level and no gap in the majority spin channel, resulting in complete spin polarization at the Fermi level [1–3]. Indeed, point-contact Andreev reflection measurements have provided conclusive evidence for its half-metallicity, with a spin polarization value as high as 98.4% being reported [4, 5]. The high degree of spin polarization, together with a reasonably high Curie temperature of 390 K, makes CrO_2 an attractive candidate for use in magnetoelectronic devices such as magnetic tunneling junctions and spin valves. For these applications it is very important to understand and control the switching behavior of the magnetic layers in the structure.

In this chapter we present results on the magnetic anisotropy of epitaxial CrO_2 films grown on (100)-TiO_2 substrates as a function of different surface treatment conditions. The substrate cleaning procedure used prior to CrO_2 film growth plays an essential role in determining its growth morphology and the resulting magnetic switching characteristics. This results primarily from the effect of strain that influ-

[*] Corresponding author: e-mail: gxmiao@mit.edu, Phone: +1 205 348 2507, Fax: +1 205 348 2346

ences the magnetic anisotropy of the film. This strain effect can be exploited for the growth of multilayer structures with different switching fields for the individual layers, or even with the layers having mutually perpendicular magnetic anisotropy directions. In contrast to the standard approaches of modifying the growth conditions and film thickness to achieve variations in the coercive field (H_c), the use of surface treatment methods as described here offer several advantages, particularly for epitaxial structures.

2 Experimental

CrO_2 has a tetragonal rutile crystal structure ($a = 4.421$ Å, $c = 2.916$ Å) that is isostructural with the rutile phase of TiO_2 ($a = 4.594$ Å, $c = 2.958$ Å). For the growth of CrO_2 films on (100)-oriented single crystal TiO_2 substrate, the lattice mismatch is anisotropic, being –3.77% and –1.42% along the [001] and [010] directions, respectively. We are able to grow epitaxial CrO_2 films on (100)-oriented TiO_2 substrates by chemical vapor deposition (CVD) using chromium trioxide (CrO_3) as a precursor. Details of the CVD growth have been reported previously [6]. In brief, oxygen is used as a carrier gas in a two-zone furnace to transport the precursor from the source region to the reaction zone where it decomposes selectively on the substrate to form CrO_2. The films are grown at a substrate temperature of about 400 °C, with the source temperature maintained at 260 °C, and an oxygen flow rate of 100 sccm. The films have been extensively characterized using atomic force microscopy (AFM) and X-ray diffraction. In order to determine the unit cell lattice parameters as a function of film thickness we have carried out X-ray diffraction measurements at angles both around the (200) normal Bragg peak and also the off-axis (110) and (101) peaks. Magnetic measurements have been performed using a Quantum Design superconducting quantum interference device (SQUID) magnetometer and a vibrating sample magnetometer (VSM). While the SQUID has been used primarily for the temperature-dependent studies, the angular dependence of the hysteresis loops at room temperature is measured using the VSM. For the magnetic measurements, it is essential that the backside and edges of the substrates are carefully cleaned to avoid unwanted contributions to the magnetic signal from deposited material on these surfaces.

3 Results and discussion

3.1 Film structure and morphology

The growth morphology of the CrO_2 films is critically dependent on the TiO_2 substrate cleaning procedure utilized prior to deposition. Films grown on as-purchased polished (100)-TiO_2 substrates that are cleaned with organic solvents (acetone and isopropanol) and then rinsed in distilled water are relatively

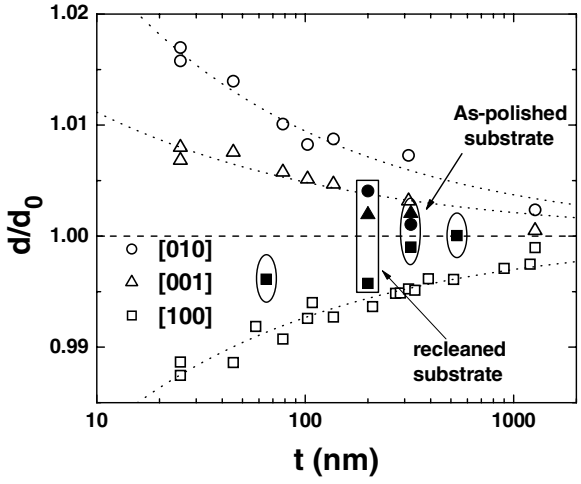

Fig. 1 Lattice parameters for epitaxial type B (open symbols) CrO_2 films as a function of thickness. Dashed lines are power law fittings, with the exponent being approximately 0.38. The lattice parameters for type A films of a few select thicknesses are shown as closed symbols.

rough and have a columnar morphology with little residual strain. The strain effect is much more pronounced in films grown on substrates that, in addition to the organic clean described above, are briefly treated with dilute HF and then water rinsed and dried prior to deposition. Hereafter, we refer to the CrO_2 films grown on TiO_2 substrates that do not or do undergo the additional HF treatment as films of type A and B, respectively. The normalized lattice parameters of CrO_2 films as a function of thickness, as determined from normal and off-axis X-ray measurements, are plotted in Fig. 1 for both the type A and type B samples. It is clear from the data that the type A films are nearly strain-free. On the other hand, the type B films exhibit a strong influence of strain that varies with thickness, with the lattice parameters gradually approaching the bulk values for the thicker layers.

The surface morphology of the substrates after cleaning, and that of the films, has been characterized using AFM. Figure 2(a) and (b) shows AFM images of the TiO_2 substrate surface after only organic clean and with additional HF treatment, respectively. While the RMS roughness for both surfaces is comparable, the HF treated surface is much better ordered locally as evidenced by the appearance of atomic steps (~4 Å). AFM images of CrO_2 films grown on these surfaces are shown in Fig. 2(c) and (d). The corresponding images at a lower magnification are shown in Fig. 2(e) and (f), respectively. The type A film, which is essentially strain-free, displays very square-like grains (Fig. 2(c) and (e)). On the other hand, the strained type B film exhibits more rectangular shaped grains, with the long direction

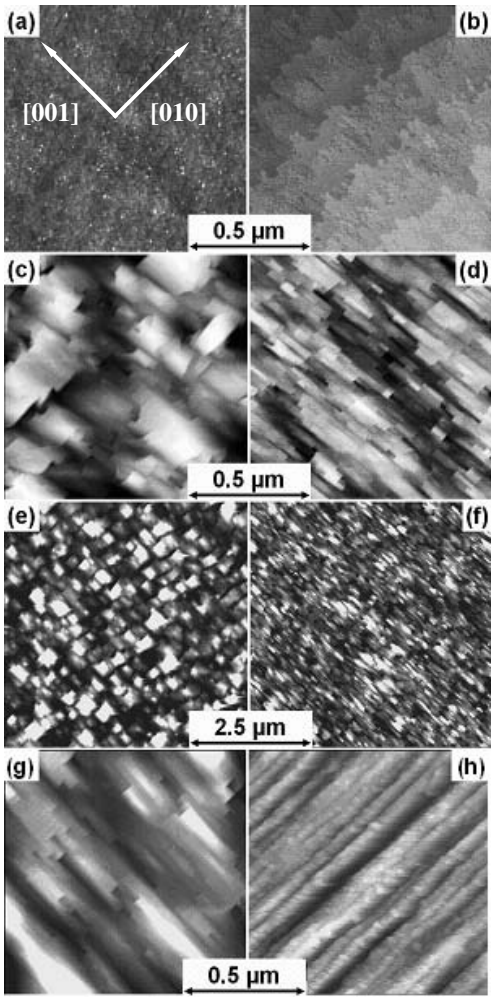

Fig. 2 Surface morphology as measured using AFM of the starting (100)-TiO_2 substrate surfaces and grown CrO_2 films. TiO_2 substrate (a) before and (b) after HF cleaning; (c) and (e) 65 nm type A CrO_2 film at different magnifications; (d) and (f) 37 nm type B film at different magnifications; (g) 85 nm type B film CrO_2 film; and (h) surface after chemical etching of film (g). The [001] and [010] directions of the substrate are marked in (a) and are the same in the other figures.

being along [001]. This suggests that the lateral growth rates in the two directions are different for the growth of the strained films, with [001] being the faster growth direction. This is consistent with the results obtained on the selective growth of CrO_2 on patterned substrates, where a strong angular dependence of the lateral growth rate is observed [7]. The different shape grains of the type A and B samples suggest that the strain in the latter might influence the relative growth rates in the two directions. The smaller lattice mismatch in the [010] direction quite likely induces lateral growth in the normal direction, i.e. along [001]. For a very crude estimate, we can assume that the lateral growth rate is proportional to the strain anisotropy energy in that direction, an aspect ratio of 2.7 is thus expected. We observe an aspect ratio of about 3 for all the type B films, independent of thickness. This indicates that the strain in the two directions is relaxed at roughly the same rate with increasing thickness, which can also be inferred from Fig. 1. On the contrary, in films that are essentially strain-free, no special growth direction is preferred, and one would expect a near unity grain aspect ratio, as is evidenced in the type A films.

3.2 Magnetic properties

Next, we focus our attention on the magnetic properties of the type A and B films. As previously noted, the type B films that grow on atomically ordered surfaces are much more heavily strained than the type A films. As we shall see this is directly reflected in their magnetic switching properties. For the strained films we describe the free energy of the system as:

$$E = K_0 + K_1 \sin^2\theta + K_2 \sin^4\theta + (K_{\sigma c} \sin^2\theta + K_{\sigma b} \cos^2\theta) = \text{const} + K_{1\text{eff}} \sin^2\theta + K_2 \sin^4\theta\,, \quad (1)$$

where K_1 and K_2 are the magnetocrystalline anisotropy energy constants; $K_{\sigma b}$ and $K_{\sigma c}$ are the strain anisotropy energy constants associated with the *b*- and *c*-axis directions, respectively; θ is the angle between the magnetization and the *c*-axis; $K_{1\text{eff}}$ is the effective anisotropy energy constant $K_{1\text{eff}} = K_1 + (K_{\sigma c} - K_{\sigma b}) = K_1 + \frac{3}{2}\lambda Y(\varepsilon_c - \varepsilon_b)$; λ is the magnetostriction coefficient; Y is the Young's modulus; and ε is the strain [8]. Since the strain is larger in the *b*-axis direction than in the *c*-axis direction due to the larger lattice mismatch, the second term in the expression for $K_{1\text{eff}}$ is negative. For very heavily strained films the effective anisotropy energy constant $K_{1\text{eff}}$ can thus be negative, resulting in an easy axis reorientation towards the *b*-axis as has been experimentally observed [9].

As seen in Fig. 1, the degree of strain in the type B epitaxial CrO_2 films is dependent on the thickness. For sufficiently thin films, the strain anisotropy can be larger than the crystalline anisotropy, and the easy axis tends to align along the *b*-axis. For thicker films, the crystalline anisotropy dominates and the easy axis is along the *c* direction as seen in Fig. 3. The critical thickness for the easy axis rotation has been determined to be at about 50 nm at room temperature. It should be noted that the values of both the crystalline and the strain anisotropy terms are temperature dependent. The former increase monotonically, almost doubling in value as the temperature is decreased from room temperature to liquid helium [10].

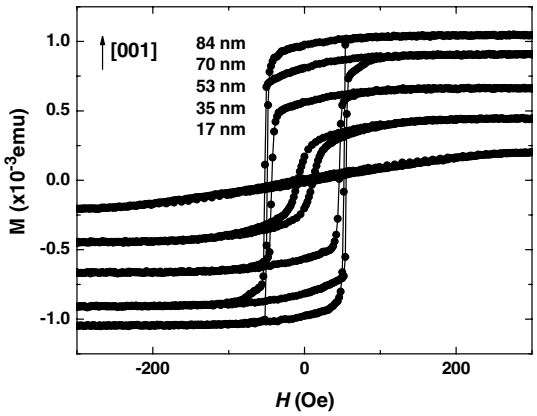

Fig. 3 Hysteresis loops displaying the evolution of the easy axis into the hard axis direction for type B (100)-oriented CrO_2 films with decreasing film thickness. The measurements for the all the films are at room temperature along the *c*-axis direction.

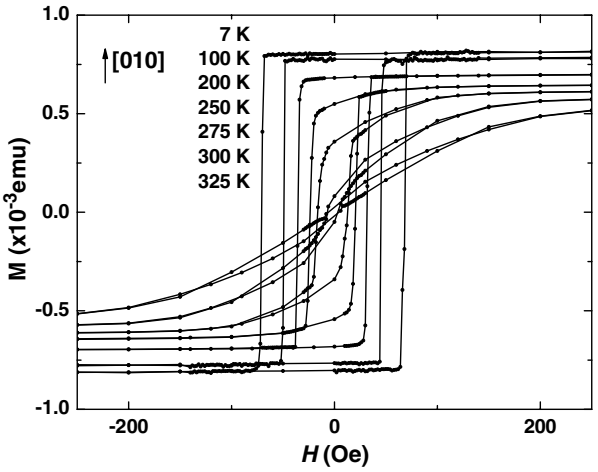

Fig. 4 Hysteresis loops displaying the evolution of the magnetic easy axis into the hard axis direction with increasing temperature for a type B film. The measurements are along the *b*-axis direction for a 47 nm film.

The strain anisotropy term is also temperature dependent through the changes of the magnetostriction coefficient, the Young's modulus and also the differences in the thermal expansion between the film and substrate. We find that an easy axis reorientation can also be achieved through changing the temperature as shown in Fig. 4, with the *b*-axis being preferred at low temperatures. Although measurements of the temperature dependence of the strain anisotropy for CrO_2 have not yet been reported, our results suggest that the temperature dependence of the product $\lambda Y\varepsilon$ is likely to be much stronger than that for K_1.

In the case of type A films, the substrate surface is rough on an atomic scale and the nucleation and growth of the film occurs quite randomly. Correspondingly, the strain anisotropy in these films is significantly smaller than the crystalline anisotropy. Because of the presence of a large number of defects the RMS roughness of these films are typically about twice as large as those of the type B films. The disorder is also reflected in the structural quality, with the (200) rocking curve width being about five times larger than that for the type B films. Despite their inferior crystalline quality, these films exhibit magnetic switching behavior close to that observed in bulk single crystals of CrO_2. Figure 5 shows the hysteresis loops of a type A and type B film, both of which are nominally 65 nm in thickness. The double switching phenomena [11], resulting from non-uniform distribution of strain, which normally appear in the type B films of intermediate thickness, is not observed in the type A films. Furthermore, because of the lack of any significant influence of strain in the latter, the magnetic anisotropy is close to being uniaxial. The magnetization is also much more uniform, resulting in a larger nucleation field. We have also

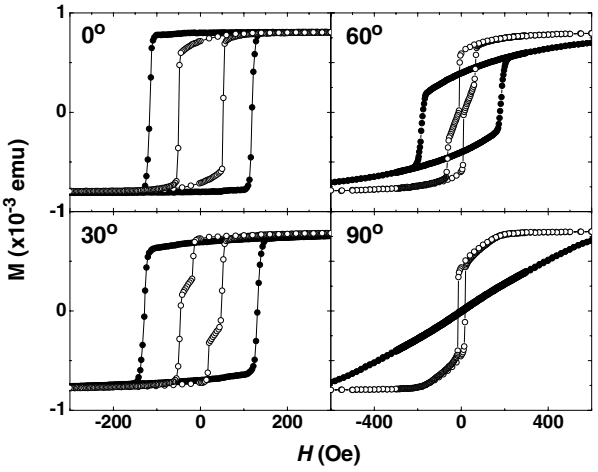

Fig. 5 Comparison of the hysteresis loops for a type A (closed circles) and a type B (open circles) CrO_2 film, both nominally 65 nm thick. The listed angles are with respect to the easy direction ([001] direction).

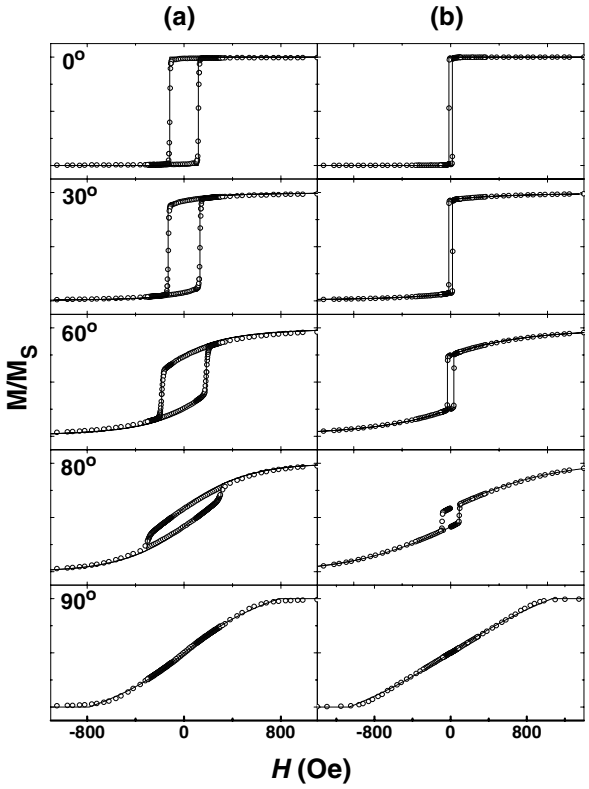

Fig. 6 Angular dependence of the hysteresis loops of type A CrO_2 films of: a) 65 nm and b) 535 nm thickness. The open circles are normalized experimental data points, while the solid lines are generated using the Stoner–Wohlfarth model except at the switching point. The K_1 and K_2 values for the fits at different angles are obtained from the hard-axis loop data.

performed ferromagnetic resonance (FMR) studies [12] on the identical set of type A and B films and the results are consistent with the results reported here using conventional magnetic measurements.

As we show in Fig. 6, the Stoner–Wohlfarth model [13] provides a very good fit for the switching of type A films of different thicknesses. This suggests that the switching in these films occurs via coherent rotation that can be described as being close to single-domain like. We have extracted the K_1 and K_2 values from the hard axis hysteresis loops and used them to generate the theoretical hysteresis curves for the other angles. The values used are, respectively, $K_1 = 13.7 \times 10^4$ erg/cm^3, $K_2 = 2.94 \times 10^4$ erg/cm^3 for the 65 nm film; and $K_1 = 22.1 \times 10^4$ erg/cm^3, $K_2 = 2.23 \times 10^4$ erg/cm^3 for the 535 nm film. The latter values are very close to the reported bulk CrO_2 anisotropy energy constants [10].

Figure 7 plots the angular dependence of the experimentally determined switching field, H_s, and the coercive field, H_c, for a 65 nm type B film. The Stoner–Wolhfarth model provides a reasonable fit for H_s only at high angles (i.e., close to the hard axis). On the other hand the Kondorskii relation [14, 15], $H_s(\varphi) = H_s(0)/|\cos\varphi|$, where φ is the angle between the applied field and c-axis, yields a more adequate fit at low angles. We find that by simply adding another parameter to this relationship, i.e.

$$H_s(\varphi) = H_s(0)\frac{b+1}{b+|\cos\varphi|}\,, \tag{2}$$

where b is a fitting parameter, a satisfactory fit can be obtained over the whole range of angles.

In addition to the HF surface treatment we have also investigated the effect of other TiO_2 substrate surface treatment procedures prior to the growth of CrO_2 films. This includes studying the influence of exposure to a low-energy ion beam. The films grown on ion beam irradiated substrates are also strained, although not to the same extent as those on HF-treated substrates. A systematic study as a function of ion beam energy and exposure time is needed in order to better understand the microscopic influence of this surface treatment procedure.

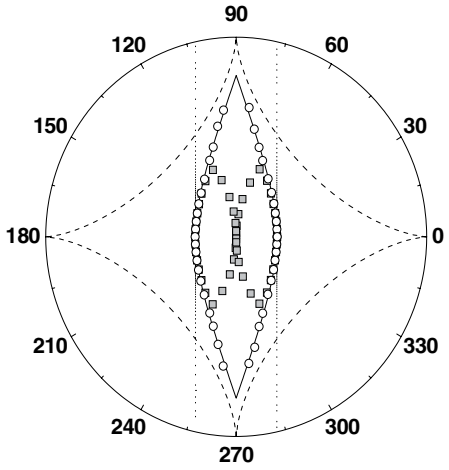

Fig. 7 Fitting of the angular dependence of the switching fields H_s (open circles) for a 65 nm type A CrO_2 film using three different models. Dashed line: Stoner–Wohlfarth model; dotted line: Kondorskii model; solid line: modified Kondorskii model, $H_s(\varphi) = H_s(0)\,\frac{b+1}{b+|\cos\varphi|}$. The squares represent the experimentally determined coercive field values, H_c.

The CrO_2 films grown on TiO_2 substrates can be readily etched off by chemical treatment using a standard chromium photomask etchant solution (e.g., from Cyantek Corp.). The cleaned substrates can then be reused (after HF pre-treatment) for subsequent growth of CrO_2 films. We find that repeatedly re-cleaned TiO_2 substrates also lead to the growth of strained CrO_2 films, but progressively less so with increasing usage as compared to virgin HF-treated substrates. This is not surprising considering that the surface becomes increasingly rougher with each deposition and surface cleaning cycle.

An alternative method of modifying the CrO_2 magnetic properties is by chemical etching (using a dilute chromium photomask etchant solution) of as-deposited films. Figure 8 shows the hysteresis loops measured at 300 and 7 K as a function of different etching time. The starting film is around 85 nm in thickness, and partial easy axis switching can be observed from its initial hysteresis loops. Chemically etching off the film gradually makes the hysteresis loops more and more "square" like in the sense that the magnetic remanence M_r/M_s becomes closer to unity with increasing etching. We find that after chemical etching, films as thin as 20 nm still retain their easy axis along the *c*-axis direction, even at low temperatures. In contrast, we have found that an as-grown 20 nm CrO_2 film will have its easy axis completely aligned along the *b*-axis, both at room temperature and at low temperatures [11]. Another impor-

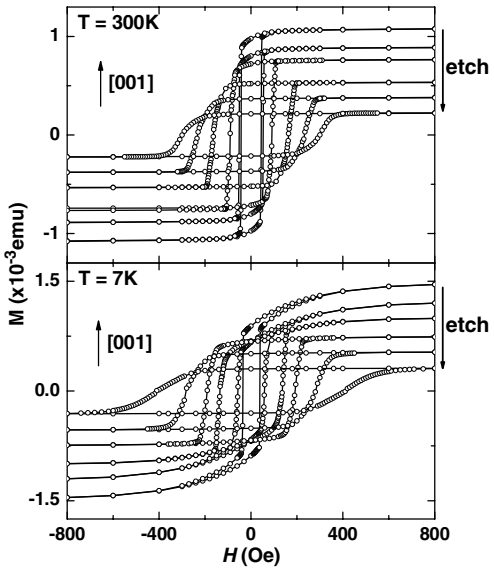

Fig. 8 Hysteresis loops at 300 and 7 K along the *c*-axis direction as a function of increasing chemical etching of a CrO_2 film, with starting thickness of about 85 nm.

tant observation is that the coercive field increases with etching time and becomes significantly large for very thin layers. This behaviour is not observed in the as-grown thin films of different thicknesses. We have noted previously that the weakly strained CrO_2 films exhibit a larger coercivity and anisotropy field than those that are more heavily strained. Thus, one possible explanation for the increase in the coercive field with etching is because of strain relaxation. Additionally, wet etching can modify the surface contribution to the total magnetization. As seen from the AFM image of an etched film (Fig. 2(h)), the etching process is very anisotropic. While the grains tend to preferentially align along the *c*-direction in the as-grown film (Fig. 2(g)), the film after etching is quite rough exhibiting periodic peaks and troughs that extend along the *b*-direction (Fig. 2(h)). This indicates the anisotropic nature of the etch process, with the etch rate being much faster in the *a*- and *b*-directions than in the *c*-direction.

Acknowledgements We thank B. Z. Rameev, L. R. Tagirov, B. Aktaş, and W. D. Doyle for valuable suggestions. This work was supported by the National Science Foundation Grant Nos. DMR-0306711, DMR-0080031 and DMR-0213985.

References

[1] K. Schwarz, J. Phys. F **16**, L211 (1986).
[2] S. P. Lewis, P. B. Allen, and T. Sasaki, Phys. Rev. B **55**, 10253 (1996).
[3] M. A. Korotin, V. I. Anisimov, D. I. Khomskii, and G. A. Sawatzky, Phys. Rev. Lett. **80**, 4305 (1998).
[4] Y. Ji, G. J. Strijkers, F. Y. Yang, C. L. Chien, J. M. Byers, A. Anguelouch, G. Xiao, and A. Gupta, Phys. Rev. Lett. **86**, 5585 (2001).
[5] A. Anguelouch, A. Gupta, G. Xiao, D. W. Abraham, Y. Ji, S. Ingvarsson, and C. L. Chien, Phys. Rev. B **64**, 180408(R) (2001).
[6] A. Gupta, X. W. Li, and G. Xiao, J. Appl. Phys. **87**, 6073 (2000).
[7] A. Gupta, X. W. Li, S. Guha, and G. Xiao, Appl. Phys. Lett. **75**, 2996 (1999).
[8] B. D. Cullity, Introduction to Magnetic Materials (Addison-Wesley, London, 1972).
[9] X. W. Li, A. Gupta, and G. Xiao, Appl. Phys. Lett. **75**, 713 (1999).
[10] D. S. Rodbell, J. Phys. Soc. Jpn. **21**, 1224 (1966).
[11] G. X. Miao, G. Xiao, and A. Gupta, Phys. Rev. B **71**, 094418 (2005).
[12] B. Z. Rameev, A. Gupta, G. X. Miao, G. Xiao, F. Yildiz, L. R. Tagirov, and B. Aktaş, phys. stat. sol. (a) **201**, 2250 (2004).
[13] E. C. Stoner and E. P. Wohlfarth, Philos. Trans. R. Soc. A **240**, 599 (1948).
[14] E. I. Kondorskii, J. Phys. SSSR **2**, 161 (1940).
[15] W. D. Doyle, J. E. Rudisill, and S. Shtrikman, J. Phys. Soc. Jpn. **17**, 567 (1962).

